Supporting Information for "Testing the Electrodynamic Method to Derive Height-Integrated Ionospheric Conductances," submitted to *Annales Geophysicae*

Daniel Weimer[1,2] and Thom Edwards[3]

[1]Center for Space Science and Engineering Research, Virginia Tech, Blacksburg, Virginia, USA
[2]National Institute of Aerospace, Hampton, Virginia, USA
[3]DTU Space, Technical University of Denmark, Copenhagen, Denmark
Correspondence: Daniel Weimer (dweimer@vt.edu)

1 Introduction

This document contains 13 additional figures that supplement those contained in the paper. Figures 1–4 in this supplement show input values and conductivity results for dipole tilt angles of $-23°$ and $+23°$ for the Interplanetary Magnetic Field (IMF) clock angles of $90°$ and $270°$, with an IMF magnitude of 10 nT. Figures 5–13 show the same maps but for an IMF magnitude

5 of 5 nT, for three dipole tilt angles ($-23°$, $0°$, $+23°$) at three IMF clock angles $90°$, $180°$, $270°$). In all figures the solar wind velocity is 450 km s^{-1} and the $F_{10.7}$ index is 160 sfu. The format is the same as Figures 4–8 in the paper.

In the top row of each figure, maps (a)-(c) shows the electric potential and the two horizontal components of the electric field. The longitudes are marked in Magnetic Local Time (MLT), in magnetic apex coordinates, with the subsolar location at 12 noon. The gray area on the maps show the region that is outside of the cap that is used in the SCHA functions in the model.

10 Minimum and maximum values of the potential and electric fields are indicated in the lower left and right corners of all contour maps, and the locations where these values are found are marked on the map with the diamond and plus symbols respectively.

In the second row of these figures, maps (d)-(f) show the equivalent current function and the duskward and sunward components of the divergence-free currents that are calculated from the gradients of this function. The color bar scale for all horizontal currents is adjusted to approximately match the largest magnitude of the sunward current.

15 In the third row, map (g) shows the field-aligned current (FAC) and (h)-(i) show the duskward and sunward components of the curl-free current. Lines are drawn only for every third interval marked on the color bar to reduce crowding around the peaks. The gray area on the maps show the region outside of the boundaries of the FAC model. The total sums of the upward (negative) and downward (positive) FAC, integrated over the spherical cap, are indicated in the upper left and right corners of the contour map in units of millions of Amperes (MA).

20 The fourth row starts with the Poynting flux, (j), calculated from the cross product of the electric and magnetic fields. The total energy flow into the ionosphere is in the upper-right corner, in Giga-watts (GW). The second map in the fourth row, (k), shows the wrong Pedersen conductivity value that would be obtained without use of the divergence-free component of the

horizontal current. Similarly, map (l) shows the wrong Hall conductivity that would be obtained if calculated without use of the curl-free current.

25   The map at the left in the bottom row, (m) shows the Joule heating that is calculated with from the dot product of the electric field and the total current. Maps (n) and (o) in the bottom row show the final values of the Pedersen conductivity and Hall conductivities, derived using the total currents. Both grey and blue areas on the maps indicate where valid conductivity values could not be computed.
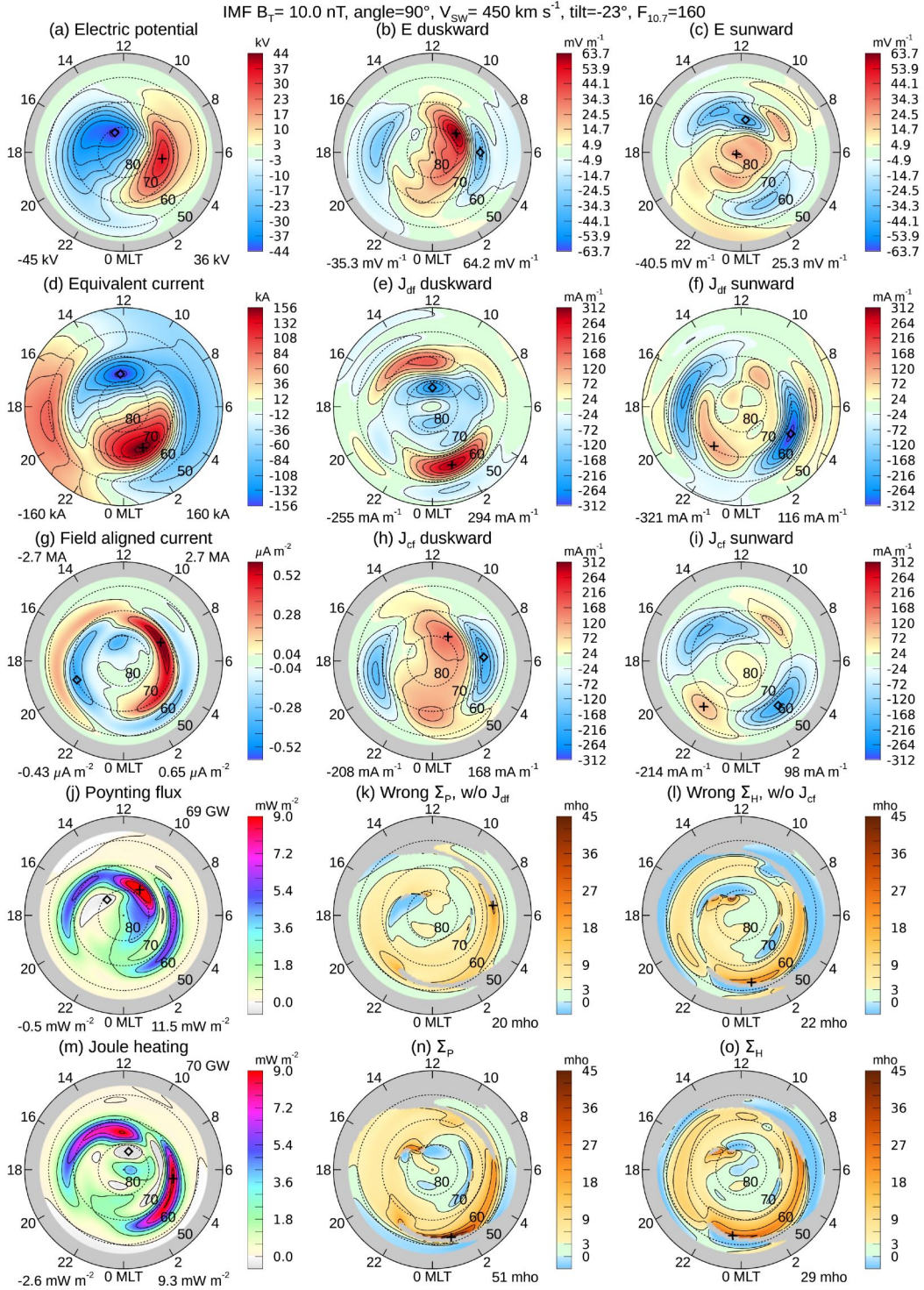
Figure 1. Conductivity input data and results, for IMF B_T magnitude 10 nT at $90°$ clock angle, and the dipole tilt angle is $-23°$.
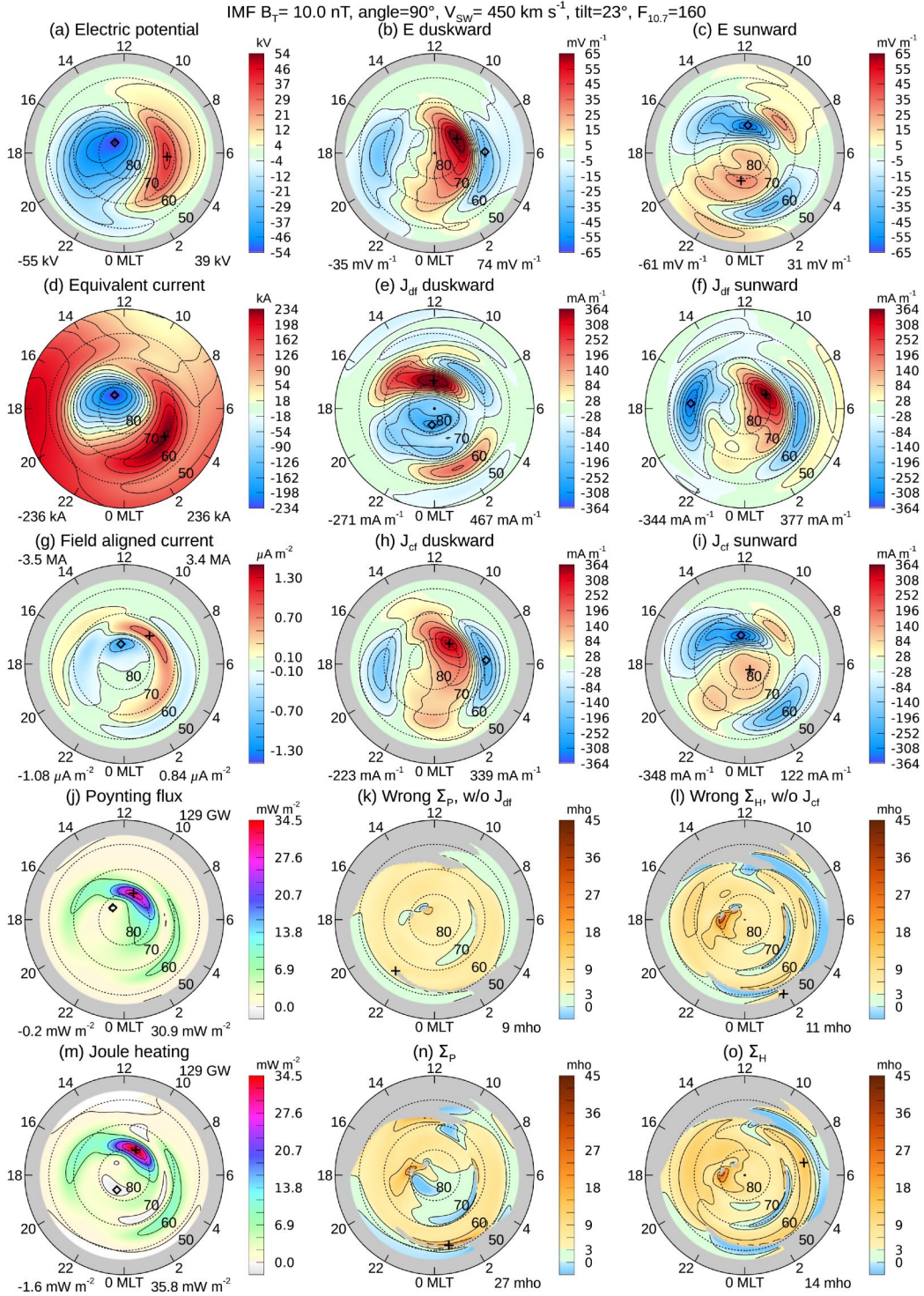
Figure 2. Conductivity input data and results, for IMF B_T magnitude 10 nT at $90°$ clock angle, and the dipole tilt angle is $+23°$.
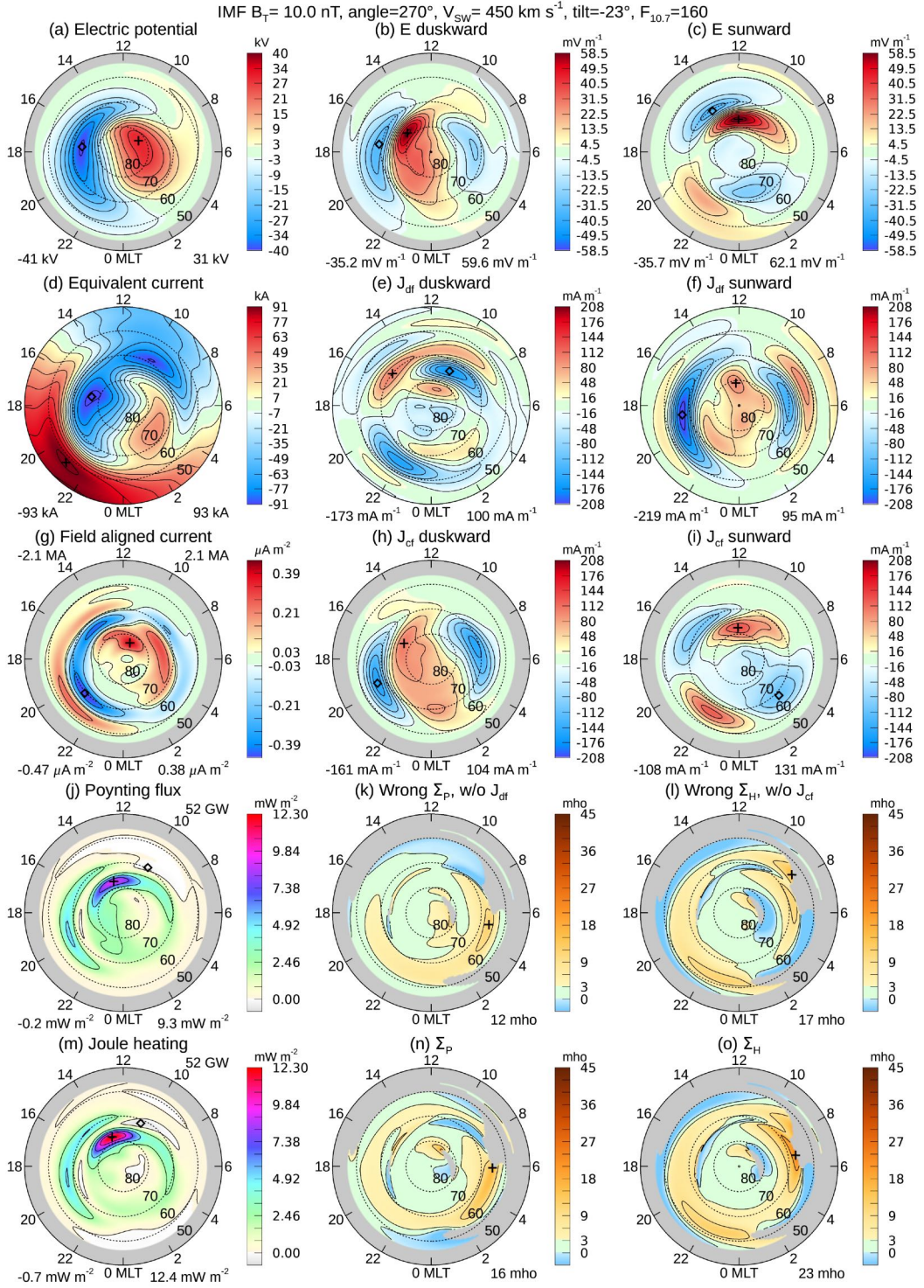
Figure 3. Conductivity input data and results, for IMF B_T magnitude 10 nT at $270°$ clock angle, and the dipole tilt angle is $-23°$.
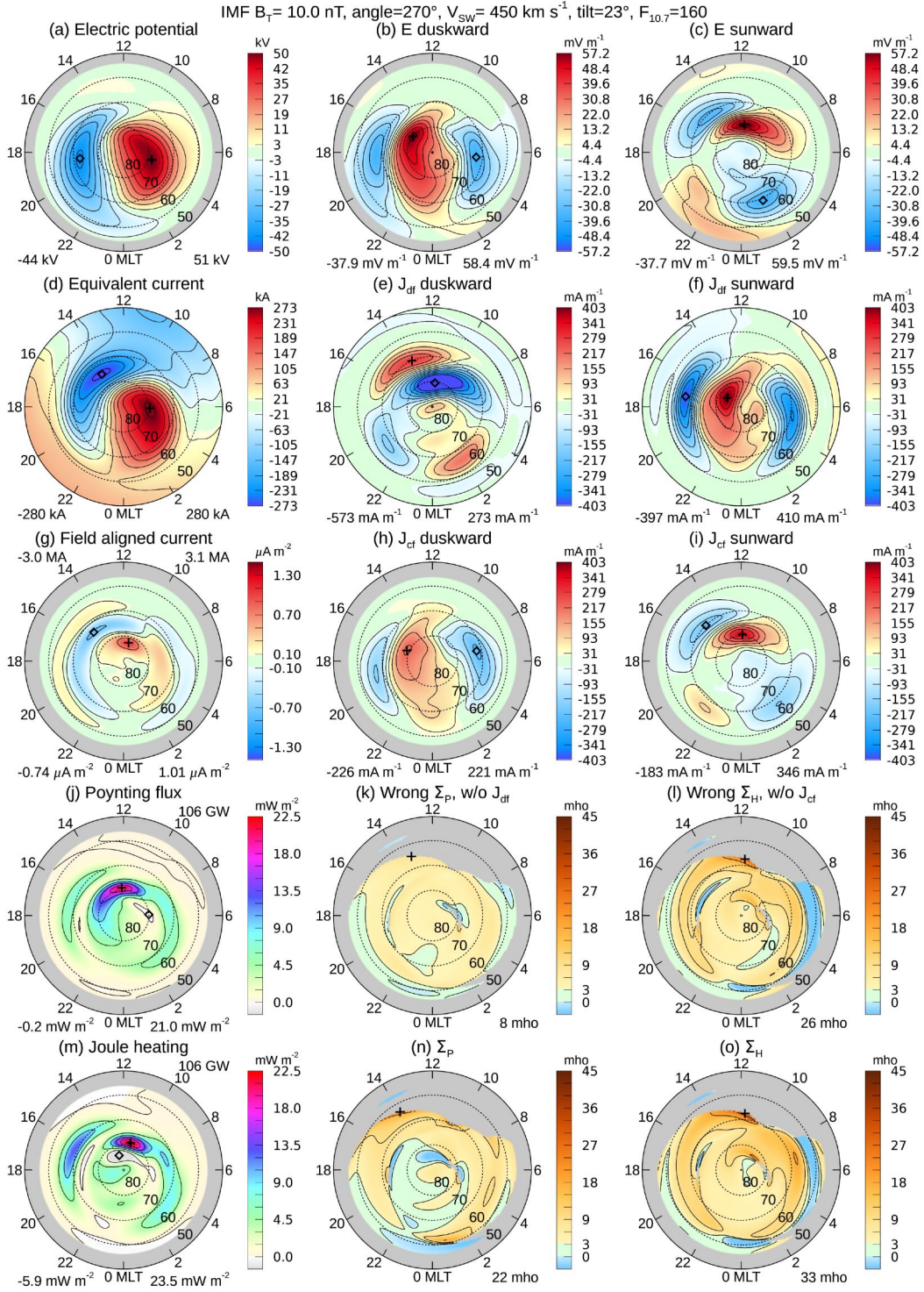
Figure 4. Conductivity input data and results, for IMF B_T magnitude 10 nT at $270°$ clock angle, and the dipole tilt angle is $+23°$.
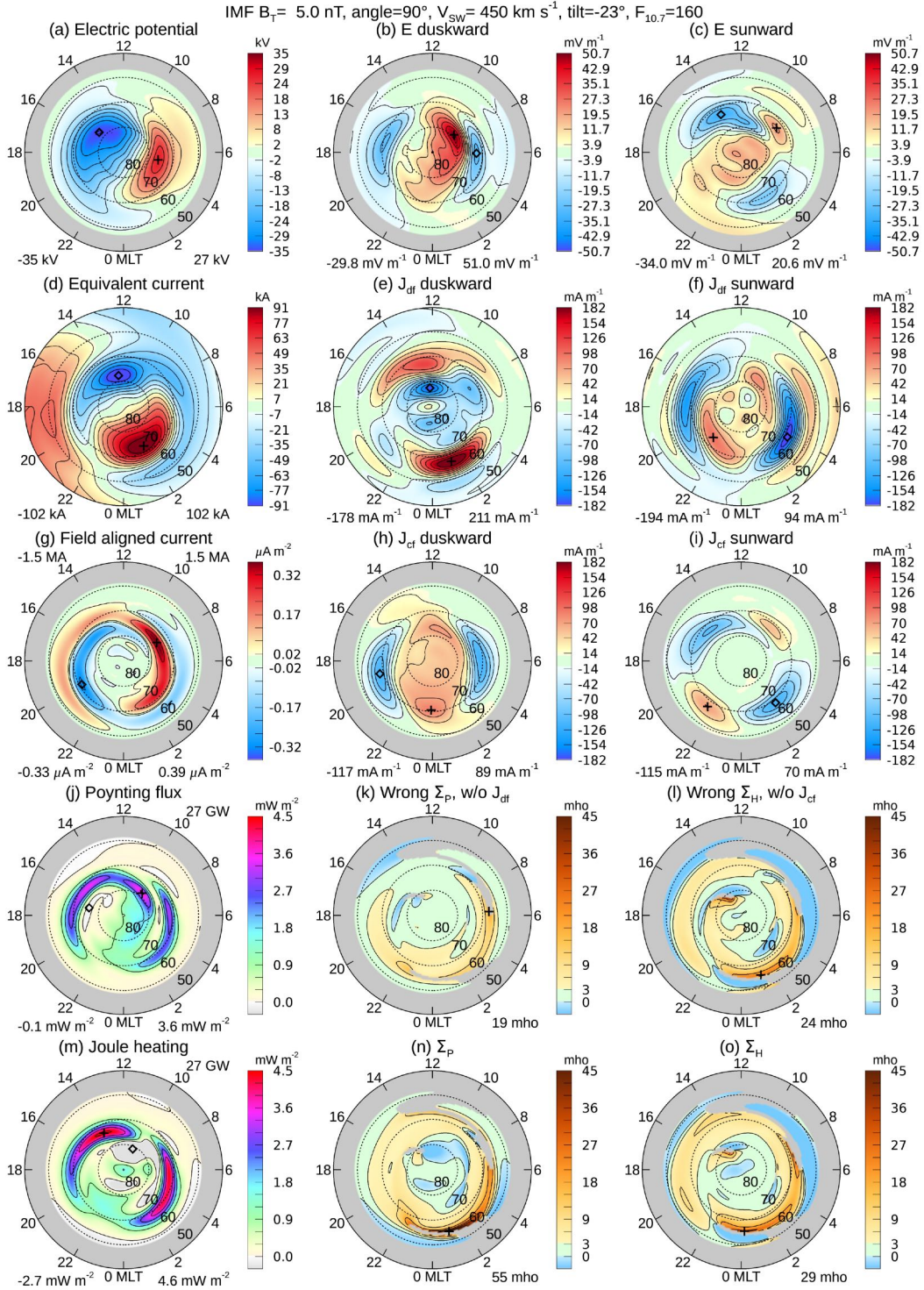
Figure 5. Conductivity input data and results, for IMF B_T magnitude 5 nT at $90°$ clock angle, and the dipole tilt angle is $-23°$.
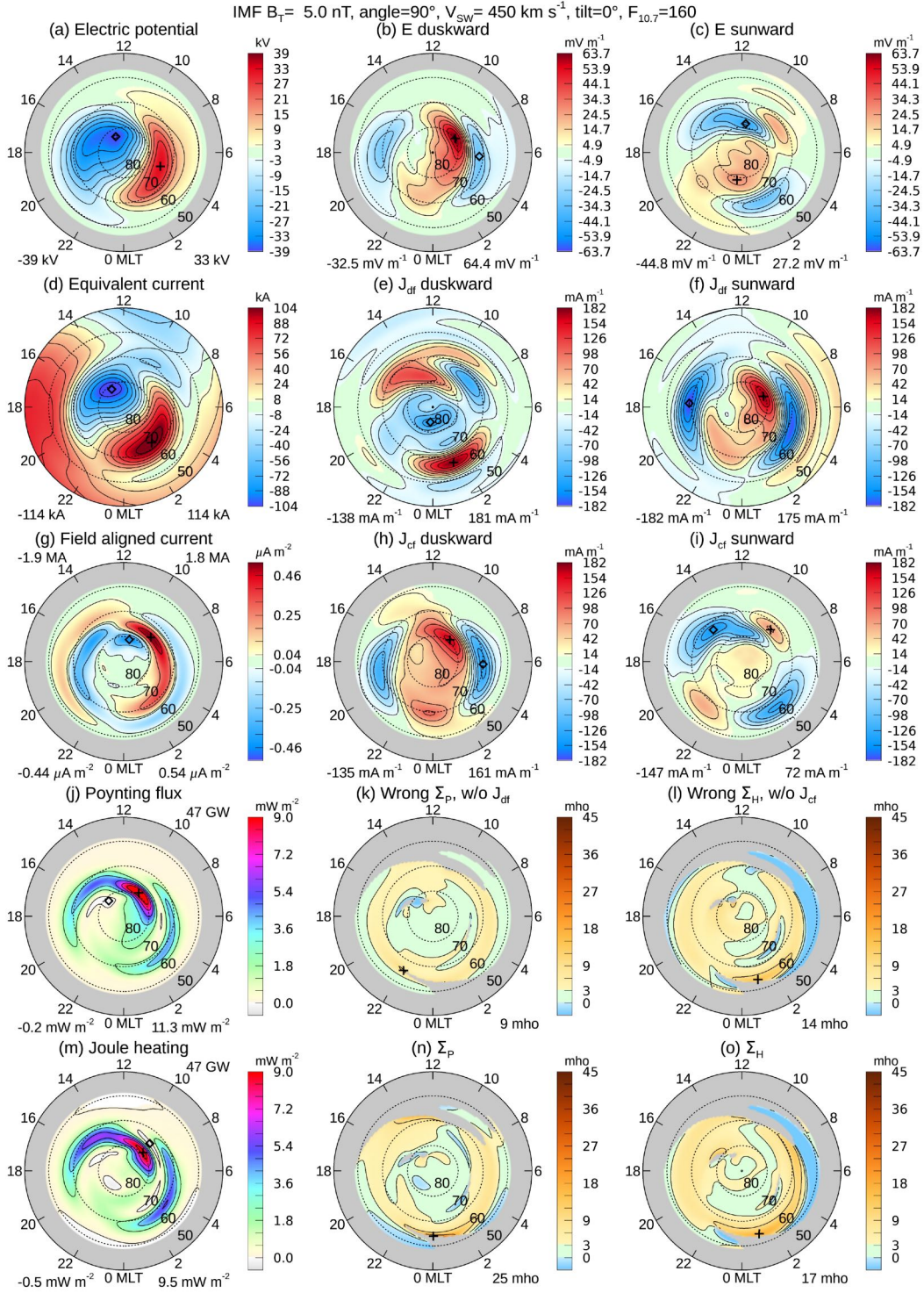
Figure 6. Conductivity input data and results, for IMF B_T magnitude 5 nT at $90°$ clock angle, and the dipole tilt angle is $0°$.
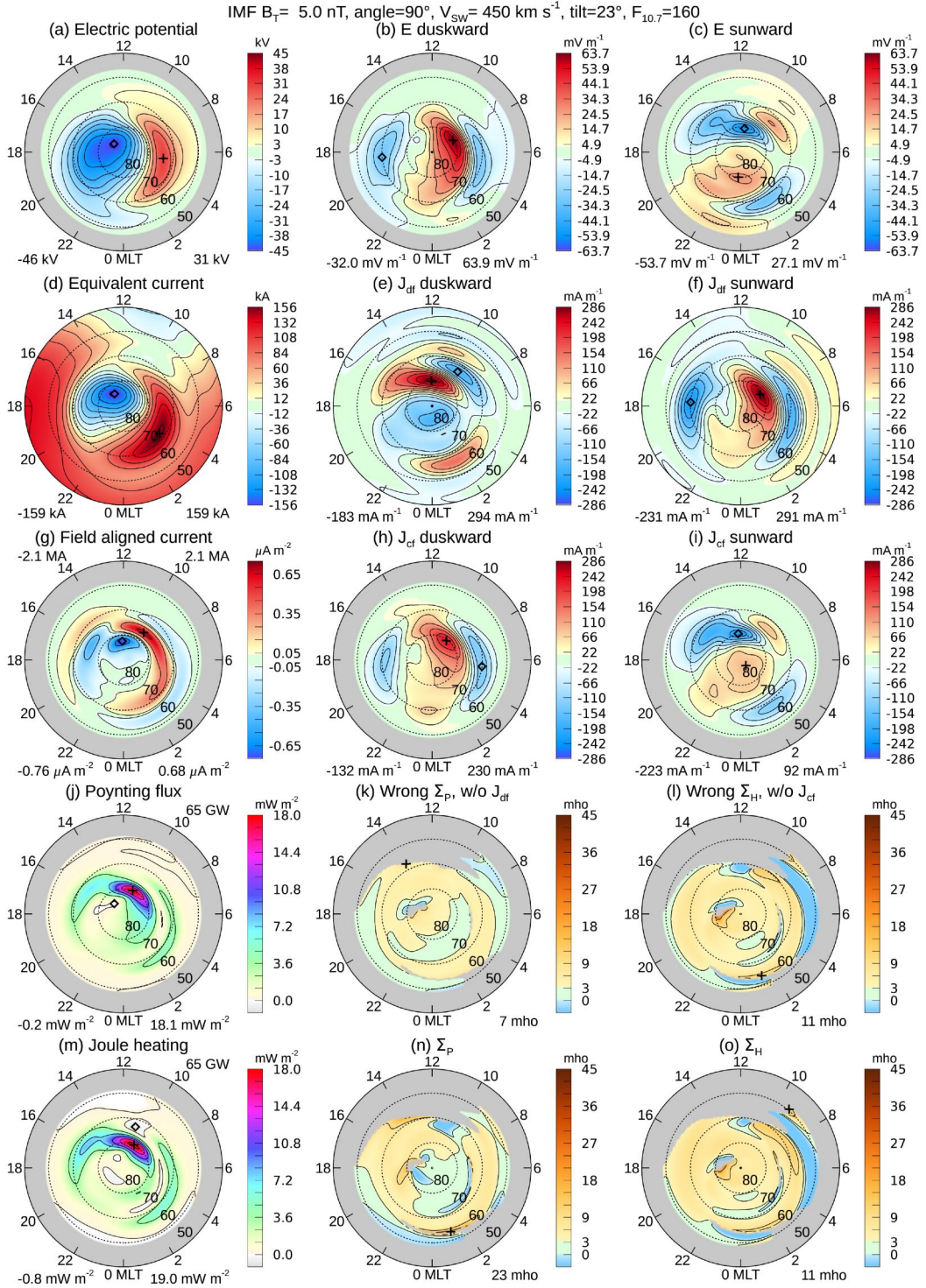
Figure 7. Conductivity input data and results, for IMF B_T magnitude 5 nT at $90°$ clock angle, and the dipole tilt angle is $+23°$.
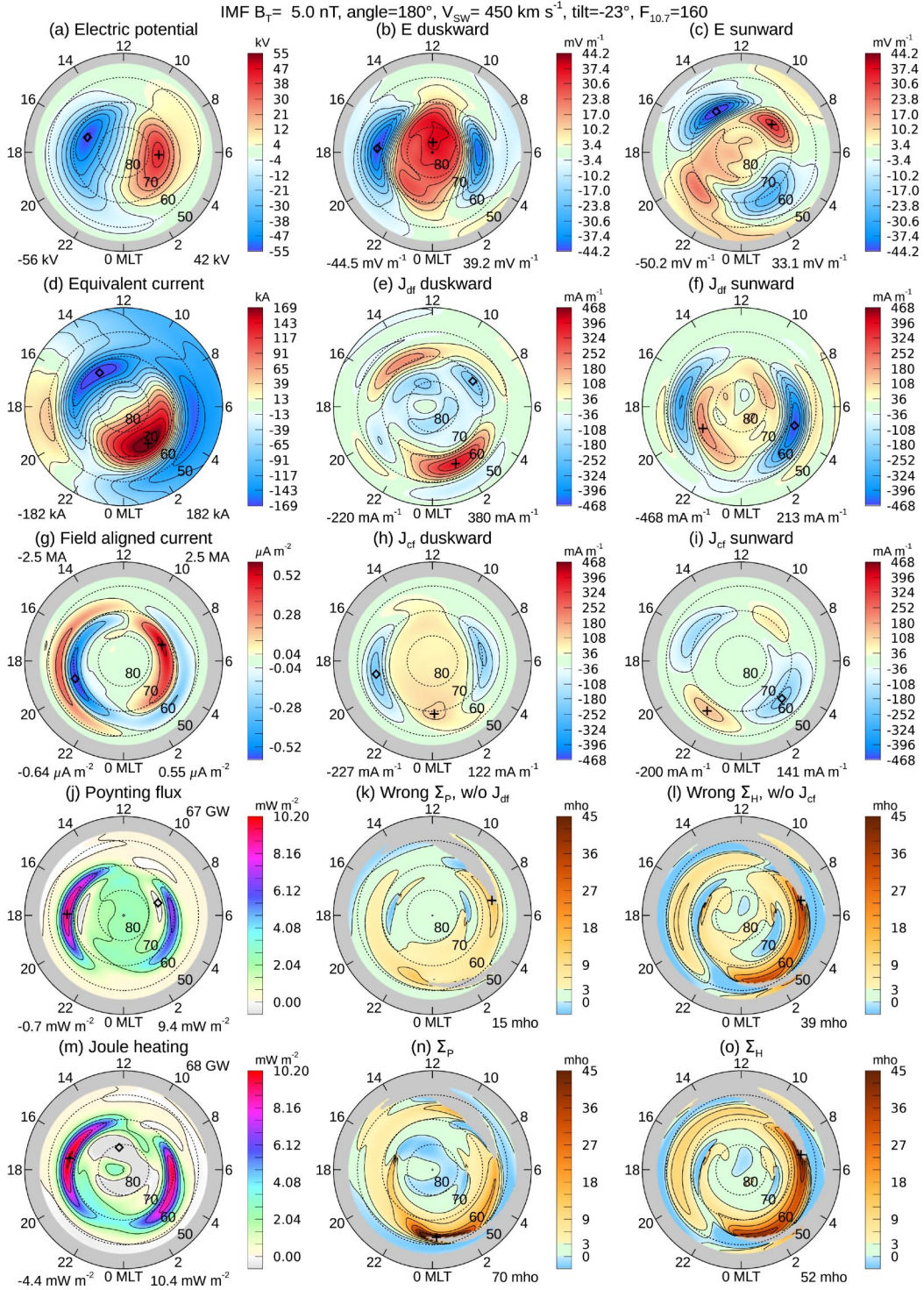
Figure 8. Conductivity input data and results, for IMF B_T magnitude 5 nT at $180°$ clock angle, and the dipole tilt angle is $-23°$.
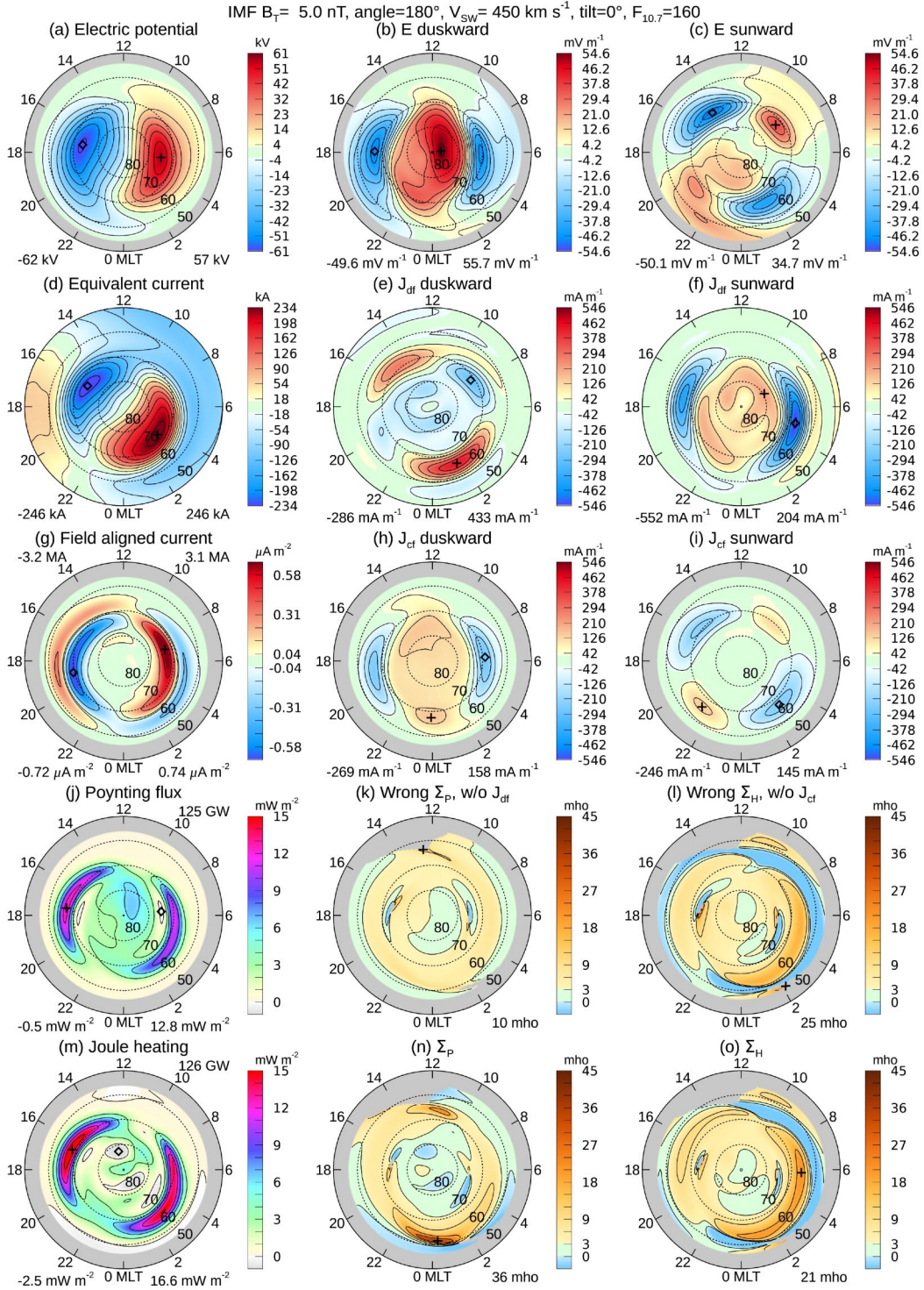
Figure 9. Conductivity input data and results, for IMF B_T magnitude 5 nT at $180°$ clock angle, and the dipole tilt angle is $0°$.
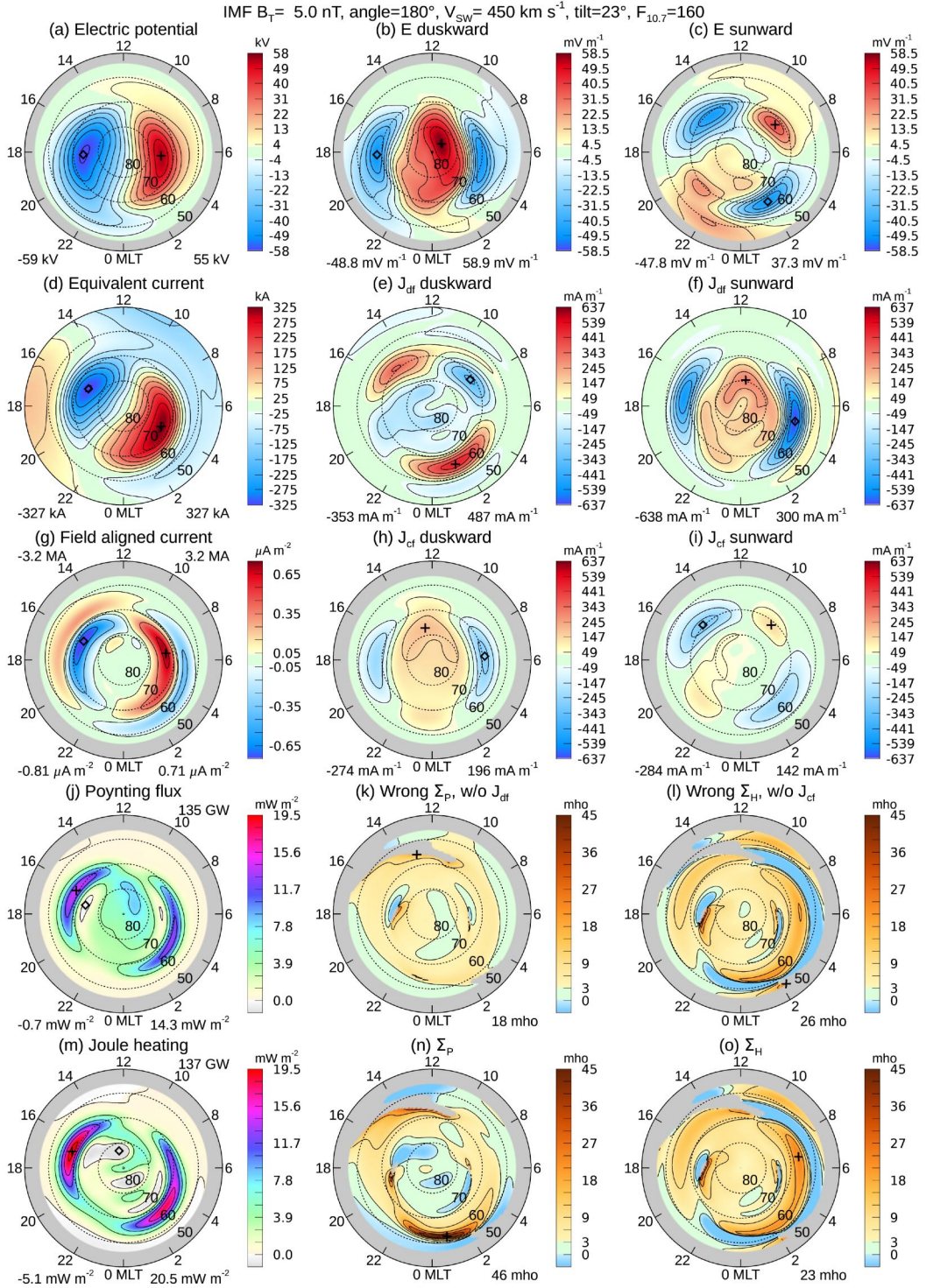
Figure 10. Conductivity input data and results, for IMF B_T magnitude 5 nT at $180°$ clock angle, and the dipole tilt angle is $+23°$.

IMF B_T= 5.0 nT, angle=270°, V_{SW}= 450 km s^{-1}, tilt=-23°, $F_{10.7}$=160
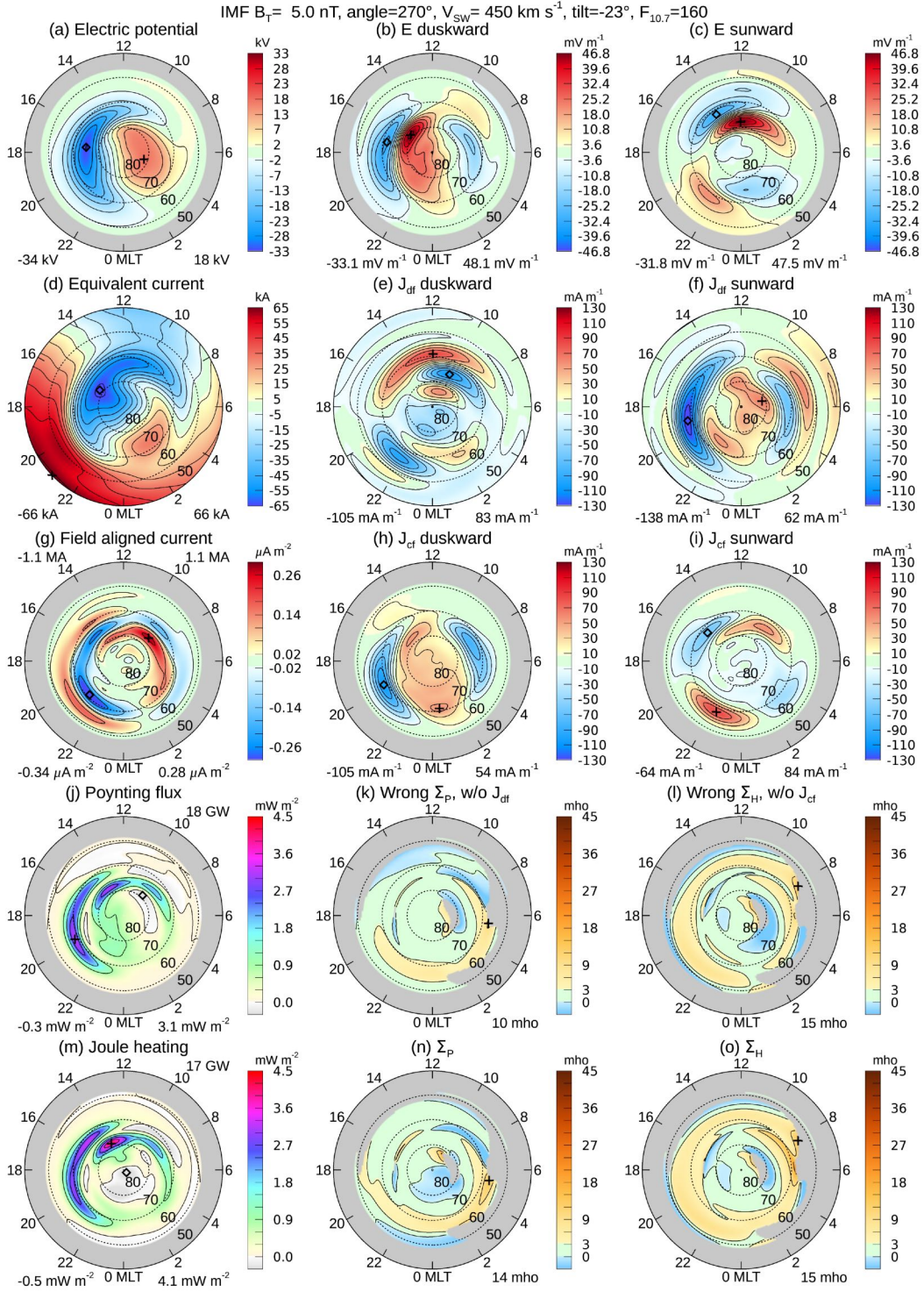
Figure 11. Conductivity input data and results, for IMF B_T magnitude 5 nT at $270°$ clock angle, and the dipole tilt angle is $-23°$.

IMF B_T = 5.0 nT, angle=270°, V_{SW} = 450 km s^{-1}, tilt=0°, $F_{10.7}$=160
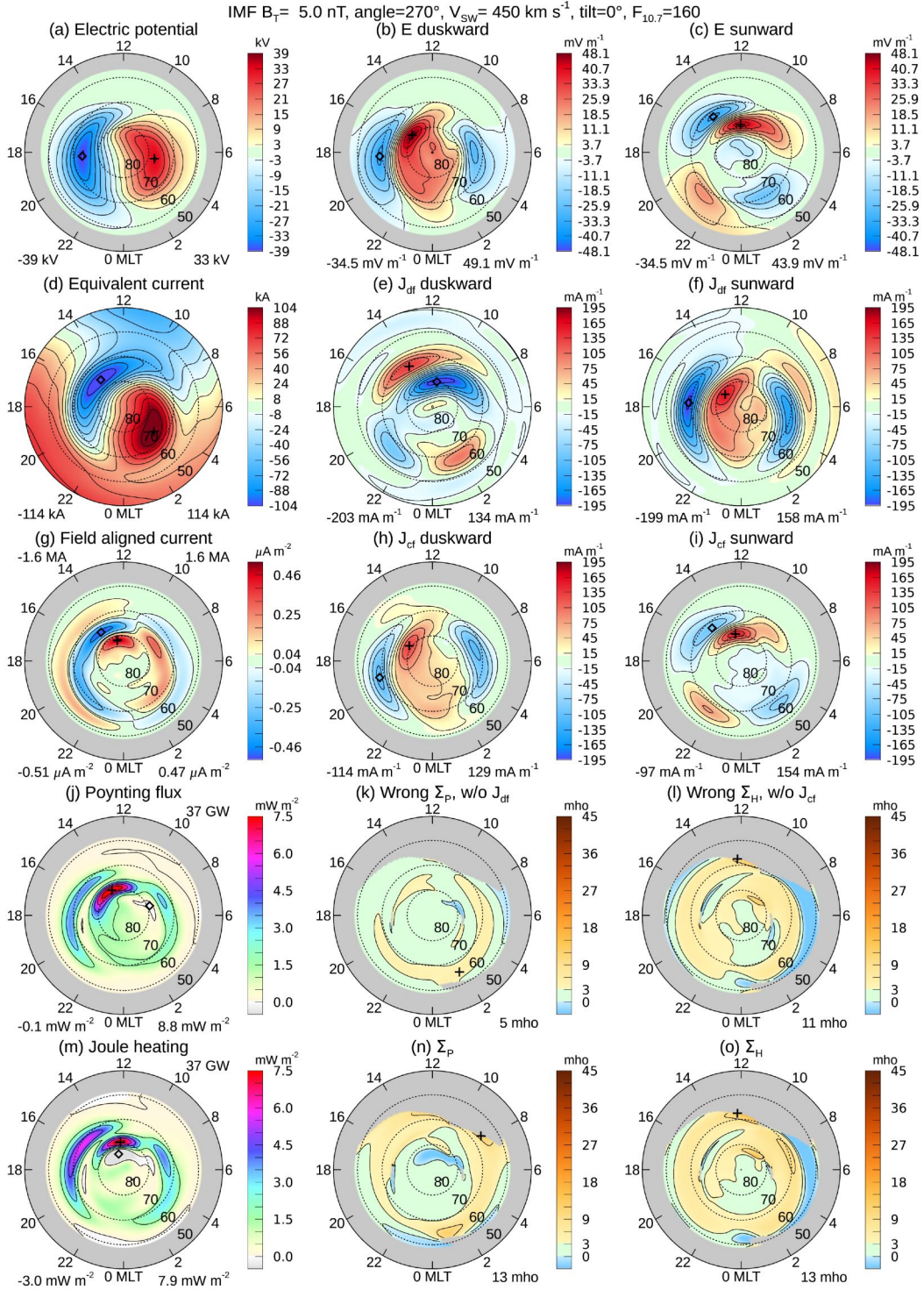
Figure 12. Conductivity input data and results, for IMF B_T magnitude 5 nT at $270°$ clock angle, and the dipole tilt angle is $0°$.
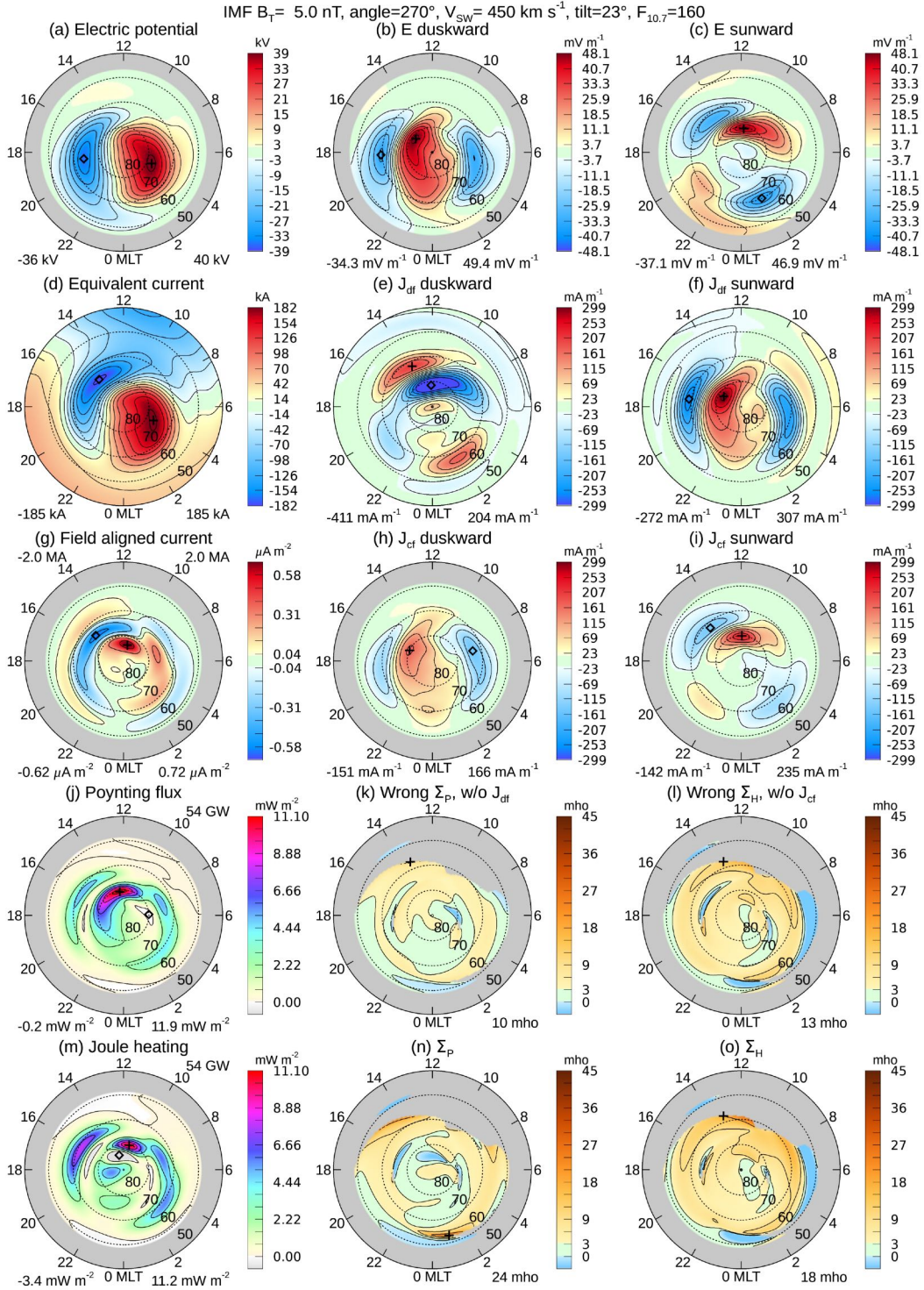
Figure 13. Conductivity input data and results, for IMF B_T magnitude 5 nT at $270°$ clock angle, and the dipole tilt angle is $+23°$.